Supporting Information

Wang et al. 10.1073/pnas.1204525109

SI Discussion

Innate immunity is essential for host defense but its dysregulation can have devastating consequences, which include unresolving inflammation, sepsis, and autoimmune disorders (1, 2). Resting phagocytes are at a quiescent state whose phagocytic and bactericidal activities are low. Upon encountering microbial products, these activities are significantly up-regulated (3–6). The mechanisms of this adaptation of the innate immune response are not well understood. Results reported here indicate that TIPE2 (TNFAIP8L2) serves as a key regulator of this process. TIPE2 is constitutively expressed at high levels in immune cells; it binds to Rac GTPases to prevent their activation and to maintain the quiescent phenotype of phagocytes. Exposure to microbes markedly down-regulates TIPE2 levels, which sets free the Rac GTPases; the free activated Rac GTPases in turn initiate their downstream effector signals, leading to enhanced innate immune responses (including phagocytosis and oxidative burst). Thus, TIPE2 serves as a negative regulator of innate immunity.

Toll-like receptors (TLRs) may enhance phagocytosis through multiple mechanisms (3–6). In addition to the TIPE2-dependent mechanism reported here, they may do so by up-regulating membrane receptors required for engulfment, intracellular signals required for cytoskeleton remodeling, and cytokines that promote phagocytosis, and so on (3–7). However, our finding that TIPE2 deficiency alone significantly altered the basal and induced levels of phagocytosis indicates that the TIPE2-dependent mechanism is essential for controlling phagocytosis. The quiescent state of phagocytes may not be maintained in the absence of TIPE2. Therefore, TIPE2-dependent regulation of innate immunity is crucial for host defense and may be targeted to promote or dampen antimicrobial immune responses.

Rac proteins are members of the Rho family of small GTPases. They are activated by guanine nucleotide exchange factors (GEFs), e.g., Dock180, and inactivated by GTPase-activating proteins (GAPs), e.g., RacGAP (8). Additionally, they can also be regulated by Rho GDP-dissociation inhibitors (RhoGDIs), which include RhoGDIα, RhoGDIβ, and RhoGDIγ (9). RhoGDIs can inhibit Rac activation by extracting prenylated GDP:Rac-GTPases from membranes and by preventing the exchange of GTP for GDP. Paradoxically, RhoGDIs also prevent the degradation of Rac proteins, thereby enhancing their activities (9–11). The roles of RhoGDIs in phagocytosis and oxidative burst are not clear because mice deficient in them do not exhibit notable abnormalities in these processes (12–14). Results reported here indicate that TIPE2 represents a unique class of Rac inhibitors, distinct from the aforementioned regulators. Although TIPE2 exhibits Rac inhibitory activity similar to that of RhoGDIs, it is not required for maintaining Rac protein stability, a well-known function of RhoGDIs (12–14). On the other hand, TIPE2, but not RhoGDIs, is essential for controlling innate immunity. However, TIPE2 may use mechanisms similar to those of RhoGDIs to inhibit Rac function. It binds to the GDP and GTP forms of Rac and prevents their membrane translocation and function. Therefore, because of the potential functional overlap between TIPE2 and RhoGDIs, it is plausible that combined deficiency in both classes of Rac inhibitors may lead to more dramatic abnormalities.

Rac proteins are over 90% identical in their sequences. They differ primarily in the C-terminal polybasic region. For example, this region in Rac1 is composed of six basic amino acids (i.e., KKRKRK), whereas in Rac2, three of these are replaced by neutral amino acids (i.e., PQQKRP). Our finding that polybasic region (PBR) deletion did not affect TIPE2-Rac binding, but Cys-189 mutation did, explains why TIPE2 is able to interact with more than one Rac protein. Cys-189 is subjected to posttranslational modifications such as prenylation and carboxymethylation, which are essential for Rac membrane translocation and activation. Our finding that TIPE2 binds to this site may explain the inhibitory effect of TIPE2 on Rac. However, among the five deletional Rac1 mutants we generated, two (with amino acids 48–123 deletion and amino acids 136–161 deletion, respectively) were unstable in cells and therefore were not further studied. Whether these corresponding regions are involved in TIPE2-Rac interaction or the inhibitory function of TIPE2 is unclear.

Our previous studies showed that TIPE2 knockout 129 mice were hypersensitive to septic shock (15). A sharp decline in the survival rate and a significant increase in seral inflammatory cytokines were observed in lipopolysaccharide (LPS)-treated TIPE2 knockout mice. In this study, TIPE2 knockout C57Bl/6 (B6) mice exhibited resistance to *Listeria monocytogenes* challenge. Unlike LPS, the endotoxin of Gram-negative bacteria, *L. monocytogenes* is an intracellular bacterium, which can invade various types of cells, including epithelial cells, hepatocytes, endothelial cells, fibroblasts, and macrophages. After entering host cells, *L. monocytogenes* is trapped temporarily in the phagosome. If the bacterium cannot be killed immediately, it will escape from the phagosome and enter the cytoplasm, where it undergoes rapid replication. Enhanced phagocytosis and reactive oxygen species (ROS) production in TIPE2 knockout mice may prevent the escape of the bacterium from the phagosome, thus inhibiting its propagation in the cytoplasm and the spreading to other cells. This action may explain why TIPE2 knockout mice have decreased bacterial load, reduced inflammatory responses, and diminished death rate.

To date, three binding partners (caspase-8, RGL, and Rac) have been identified for TIPE2. We do not have evidence that TIPE2, Rac, RGL, and caspase-8 are in a single complex. The interesting thing is that these binding partners control similar downstream signal pathways and therefore their regulation by TIPE2 may lead to similar outcomes. For example, AKT and the c-Jun N-terminal kinase (JNK) pathways may be regulated by all of the known TIPE2-binding proteins. By targeting several signaling pathways that play related roles, TIPE2 may more effectively control complex cellular processes such as phagocytosis and survival than by targeting only a single pathway.

SI Methods

Mice. Wild-type B6 and C57BL/6-Tg(UBC-GFP)30Scha/J mice were obtained from the Jackson Laboratory. C57BL/6 mice that carry a *Tipe2* gene null mutation were generated by backcrossing *Tipe2*$^{-/-}$ 129 mice (15) to B6 mice for 12 generations. All animal procedures were preapproved by the Institutional Animal Care and Use Committee of the University of Pennsylvania.

Plasmid Constructs. Full-length TIPE2 was generated from the cDNA clone by PCR and cloned in frame with an N-terminal Flag into vector pRK5. pEGFP-TIPE2 was generated by cloning an amplified TIPE2 fragment into vector pEGFP-N3. Human wild-type Rac1, Rac1 T17N, Rac1 Q61L, and Rac2 cDNAs were obtained from Addgene and subcloned into pRK5 with Myc or HA tag at the N terminus. The mutant Rac1 (C189S), TIPE2 (K15/16Q), TIPE2 (K20A), and TIPE2 (R24A) were generated by PCR-based site-directed mutagenesis. Truncated forms of Rac1 lacking the N-terminal amino acids 1–47 and C-terminal amino acids 162–192 or 189–192 were generated from the cDNA clone by PCR with appropriate primers and cloned in-frame with an N-terminal HA tag

into vector pRK5. Human HRas G12V cDNA was obtained from Addgene. cDNAs encoding TIPE2, wild-type Rac1, Rac1 T17N and Rac1 Q61L, and HRas G12V were subcloned into the murine stem cell virus (MSCV)-based retroviral vector that coexpresses the truncated human nerve growth factor receptor (NGFR).

Cell Culture and Transfection. The murine RAW264.7 macrophages (ATCC) and HEK293T cells (ATCC) were cultured in DMEM containing 10% (vol/vol) heat-inactivated FBS, 2mM L-glutamine, and 100 units/mL penicillin/streptomycin (D10). Transfections were performed using Lipofectamine LTX according to the manufacturer's instructions (Invitrogen).

Macrophage Generation and Neutrophil Isolation. To generate bone marrow-derived macrophages (BMDMs), bone marrow cells were harvested from mice and cultured for 7 d in 30% L-929 cell culture supernatant and 70% D10. Cells were washed twice with cold DPBS and collected with 5 mM EDTA in DPBS. After centrifugation, they were resuspended in D10 and rested for 24 h before functional assays. BMDMs were >95% $CD11b^+$ and $F4/80^+$ as determined by flow cytometry. Morphologically mature neutrophils were purified from murine bone marrow by Percoll gradient centrifugation, as previously described (16). Briefly, bone marrow cells were harvested from mice using neutrophil isolation buffer (1× HBSS without Ca^{2+} and Mg^{2+} containing 0.25% BSA). After RBC lysis, cells were layered on a three-step Percoll gradient (81%, 62%, 55%). Following centrifugation at 1,200 × *g* for 30 min at room temperature, cells at the 81%:62% interface were removed and washed once with the isolation buffer before being used in the experiment. Neutrophil viability was >95% according to the results from trypan blue staining. Purity was typically ~75–85% as assessed by flow cytometry based on the forward and side scatter and high Gr1 staining.

Gene Transfer in Primary Macrophages. To produce retroviruses, packaging cells (293T) were cultured in 6-cm culture dishes with D10 and transfected with NGFR MSCV-based retroviral vector containing the gene of interest along with pVSVG and pCGP sequences, using the CalPhos mammalian transfection kit (Clontech). The transfection medium was replaced with fresh medium 6 h posttransfection. Forty-eight hours later, the culture medium containing recombinant retroviruses was harvested and filtered (0.45 μm). Bone marrow cells were isolated from WT and $Tipe2^{-/-}$ mice and cultured in 70% D10 and 30% L-929 cell culture supernatant. The cells were infected with retroviruses at day 2 and day 3 and allowed to differentiate into BMDMs. The infection efficiency was ~10% as determined by FACS analysis (for $NGFR^+$ cells) at day 7 of the culture.

Microbial Strains and Infection. Wild-type and hly^- mutant *L. monocytogenes* (10403s) were provided by H. Shen and Y. Paterson (University of Pennsylvania). *L. monocytogenes*, *Escherichia coli* (strain DH5a), and *Staphylococcus aureus* (ATCC 29213) were grown at 37 °C in brain-heart-infusion medium (Becton Dickinson), Luria–Bertani medium (Fisher), and Columbia medium with 2% NaCl, respectively. For all assays, midlog-phase bacteria were used. Bacterial in vitro infection was assayed in 12-well plates. A total of 5×10^5 BMDMs or 2×10^5 Raw264.7 cells were seeded in each well, followed by culturing overnight in DMEM with 10% FBS. Cells were infected with *L. monocytogenes* or *E. coli* at multiplicity of infection (MOI) of 5 or 10. Synchronous infection conditions and an enhanced bacterium–host cell interaction were achieved by a 2-min centrifugation (500 × *g*). The end of the centrifugation was considered the starting point of infection. Fifteen minutes after the inoculation, cells were washed three times with PBS, and fresh medium containing gentamycin (30 μg/mL) was added. At various time points, cells were washed and lysed with buffer for RNA or protein extraction.

For in vivo bacterial infection, *L. monocytogenes* was grown in brain-heart-infusion medium until the absorbance at 600 nm reached 0.1 of optical density. *S. aureus* was grown in Columbia media with 2% NaCl. Six- to 7-wk old $Tipe2^{+/+}$ and $Tipe2^{-/-}$ mice were infected i.v. with 2×10^5 *L. monocytogenes* in 200 μL PBS or ~$2–6 \times 10^7$ *S. aureus* in 200 μL saline. For measurement of the bacterial burden in liver and spleen, mice were killed 24 or 72 h after inoculation, organs were homogenized in 0.1% Triton in PBS, and serial dilutions of the homogenate were plated on brain-heart-infusion agar plates or Columbia Agar with 5% sheep blood plates (Becton Dickinson). The colonies were counted 24 h later. Serum alanine aminotransferase (ALT) and aspartate aminotransferase (AST) levels were determined using the Infinity ALT or AST liquid stable reagent (Thermo).

Real-Time Quantitative PCR. Total RNA was isolated using RNeasy Kits (Qiagen) primed with random hexamer oligonucleotides and reverse transcribed using Invitrogen reverse transcriptase II. Real-time quantitative PCR was carried out in an Applied Biosystems 7500 system, using Power SYBR Green PCR Master Mix (Applied Biosystems). Relative levels of gene expression were determined with GAPDH as the control. Quantitect primers for mouse GAPDH, TIPE2, IL-6, IFNβ1, and TNFα were purchased from Qiagen.

Protein Extraction, Cell Subcellular Fractionation, and Immunoblotting. Whole-cell lysate was prepared by suspending cells in the cell lysis buffer (150 mM NaCl, 10 mM Tris, pH 7.4, 0.1% SDS, 1% Triton X-100, 1% sodium deoxycholate, 100 μM Na_3VO_4, 5 mM EDTA, 1 mM PMSF) supplemented with 1× complete protease inhibitors mixture (Roche). 293T-cell membrane protein and cytoplasmic protein were prepared using a Subcellular Protein Fractionation Kit (Pierce) according to the manufacturer's instructions. A Qproteome Cell Compartment Kit (QIAGEN) was used to prepare cytosolic and membrane protein from BMDMs. Protein concentration was determined by BCA assay (Pierce). Equal quantities of proteins were separated by SDS/PAGE, transferred to a nitrocellulose membrane, and blotted with specific antibodies. The membrane was developed using Pierce SuperSignal reagent. Antibodies used were as follows: rabbit anti-TIPE2 (provided by Y. Fan, Shandong University, Jinan, China), mouse anti–β-actin and HRP-conjugated mouse anti-Flag (Sigma-Aldrich); HRP-conjugated mouse anti-Myc, HRP-conjugated mouse anti-HA, rabbit anti-Rac1/2/3, rabbit anti-integrin β1, rabbit anti-phospho-PAK1(Ser144)/PAK2 (Ser141), rabbit anti-PAK1/2/3 antibody, rabbit anti-phospho SAPK/JNK(Thr183/Tyr185), mouse anti-JNK, and rabbit anti-RhoGDI (Cell Signaling); and HRP-conjugated anti-mouse or anti-rabbit Ig (GE Healthcare).

Cell Lysate Preparation, Protein in Vitro Translation, and Immunoprecipitation. Raw cells or 293T were lysed in immunoprecipitation (IP) buffer (150 mM NaCl, 10 mM Tris, pH 7.4, 0.5% Nonidet P-40, 100 μM Na_3VO_4, 1 mM PMSF) supplemented with 1× complete protease inhibitors mixture (Roche). Extracts were assayed for protein content, using the BCA protein assay kit (Pierce) after clarification by high-speed centrifugation at 4 °C. In some experiments, in vitro translated proteins were used for immunoprecipitation. ^{35}S-labeled or unlabeled proteins were synthesized by using the TNT quickcoupled transcription/translation system from Promega according to the manufacturer's instructions. Immunoprecipitation was performed using Dynabeads protein G (Invitrogen). In brief, 1.5 mg protein-G Dynabeads was coated with 5 μg specific antibodies or Ig control for 1 h at room temperature with rotation. After removing unbound antibody, the bead–antibody complex was incubated with 500 μL cell lysate or in vitro translated protein mixture (1:4 diluted in IP buffer) for 4 h at 4 °C with rotation. The captured Dynabead/Ab/Ag complex was washed four times with PBS and boiled in 2× Laemmli buffer. The eluted proteins were

fractionated by SDS/PAGE and detected by autoradiography or Western blot.

Loading of Rac1 with GDP and GTP. The 293T cells were transiently transfected with Myc-tagged Rac1-17N or Rac1-61L for 18 h. Cells were lysed in cell lysis buffer (50 mM Tris, pH 7.5, 10 mM EDTA, 0.2 M NaCl, 0.5% Nonidet P-40, and 1× protease inhibitors mixture) (Roche). Totals of 1 mM GDPβS and 0.2 mM GTPγS (Enzo Life Sciences) were loaded to Rac1-17N– and Rac1-61L–transfected cell extracts, respectively. After 20 min incubation at 30 °C, samples were placed on ice immediately and $MgCl_2$ was added to a final concentration of 10 mM to stop nucleotide exchange.

Immunofluorescence and Confocal Microscopy. The 293T cells were grown on two- or four-well chamber slides (Lab-Tec) and transfected with GFP-tagged TIPE2 or GFP control plasmid. Eight hours after transfection, cells were fixed in 2% paraformaldehyde and permeabilized in 0.3% Triton X-100. The cells were then blocked with 4% BSA and stained with mouse anti–GTP-Rac mAb (NewEast), followed by Alexa Fluor 555-conjugated anti-mouse IgG (Invitrogen). The slides were mounted in ProLong Gold antifade reagent with DAPI (Molecular Probes). Fluorescence images were captured with a laser confocal microscope (Zeiss LSM 510META NLO microscope) at 63× magnifications.

PBD Pull-Down Assay. The 293T cells were transfected with 1.25 μg of plasmids encoding TIPE2 or HRas G12V. Empty vector was added so that the total amount of DNA used per well of the six-well plate was 2.5 μg. Eight hours after transfection, cells were washed in PBS and lysed in PBD lysis buffer (50 mM Tris, pH 7.5, 10 mM $MgCl_2$, 0.2 M NaCl, 0.5% Nonidet P-40, and 1× protease inhibitors mixture) (Roche). The lysate was incubated with 20 μg of p21-activated kinase (PAK)-GST protein beads (Cytoskeleton) for 30 min at 4 °C. After washing, protein on beads and in total cell lysates was subjected to Western blot to determine the level of active Rac. To measure Rac activity in mouse macrophages, wild-type or *Tipe2*$^{-/-}$ BMDMs were collected with 5 mM EDTA-PBS. After washing, cells were held in suspension for 1 h in 0.5% BSA and seeded on plastic dishes coated with 10 μg/mL fibronectin (Sigma-Aldrich) for 15 min at 37 °C. The levels of active Rac were determined as described above.

F-Actin Determination. F-actin content was determined by NBD-phallacidin labeling. Briefly, after LPS (100 ng/mL; Sigma-Aldrich) treatment, the cells were fixed with 3.7% formaldehyde for 15 min at room temperature and permeabilized with 0.5% Triton X-100 for 5 min. F-actin was then stained with 50 units/mL NBD-phallacidin (Molecular Probes) for 1 h at room temperature. After washing, F-actin–bound NBD-phallacidin was extracted with methanol for 1 h. Extracts were centrifuged and measured using a fluorescence plate reader with excitation and emission wavelengths set at 465 nm and 535 nm, respectively.

Phagocytosis Assay. To prepare apoptotic cells for phagocytosis assay, GFP-positive thymocytes were harvested from 3- to 4-wk-old C57BL/6-Tg(UBC-GFP)30Scha/J mice, and apoptosis was induced by incubation at 37 °C in 5% CO_2 for 5 h in the presence of 5 μM dexamethasone (Sigma-Aldrich). After dexamethasone treatment, cells were washed three times with PBS and resuspended in DMEM with 2% FBS. This treatment routinely yielded over 70% apoptotic thymocytes as measured by annexin V staining. Phagocytosis assay was performed in a 12-well nontissue culture-treated plate (BD Falcon). A total of 1×10^6 BMDMs were seeded in each well, followed by culturing overnight in DMEM with 2% FBS. GFP$^+$ apoptotic thymocytes were then added at a ratio of 5:1, and centrifugation was performed at $500 \times g$ for 2 min to synchronize binding and internalization. After 30 min of incubation at 37 °C, plates were rapidly washed two times with ice-cold PBS, and cells collected with 5 mM EDTA-PBS. Cells were then fixed with 2% paraformalhyde in PBS, stained with APC-conjugated anti-F4/80, and analyzed by flow cytometry. Gates were set for macrophages in FSC/SSC dot blots. Experiments using fluorescent latex beads (2 μm; Sigma-Aldrich) were performed in a similar fashion. For bacterial phagocytosis assay, *L. monocytogenes* were washed twice with sterile PBS and incubated (at 1×10^9/mL bacteria) in 2 μM carboxyfluorescein succinimidyl ester (CFSE) (Molecular Probes) for 20–30 min under constant shaking at 37 °C. CFSE-labeled bacteria were washed three times with PBS before being used. Live or heat-killed bacteria (70 °C for 60 min) were fed to BMDMs at a ratio of 10:1 in DMEM with 5% normal mouse serum (NMS).

Determination of Bactericidal Activity. The ability of macrophages or neutrophils to kill bacteria was measured as described in refs. 17 and 18. In brief, 2.5×10^6 cells and 2.5×10^6 bacteria were mixed with 1 mL balanced salt solution (BSS) containing 5% NMS in polypropylene snap-cap tubes (12 × 75 mm). The tubes were rotated end-over-end for 20 min at 37 °C and then centrifuged at $250 \times g$ for 8 min at 4 °C. Free bacteria were removed by three washes with 2 mL of ice-cold BSS and one additional wash with 1 mL 30% sucrose. The cells were resuspended in 1.0 mL of BBS/5% NMS. A 0.1-mL sample was removed for enumeration of the baseline infection rate for each sample. The remaining 0.9-mL samples were further incubated for another 120 min at 37 °C and then bacterial colonies quantitated. Macrophages were lysed in sterilized Millipore water (pH 8.0), and water at pH 11 was used to lyse neutrophils. Bactericidal activity was calculated by comparing cfus before and after the 120-min incubation. The killing rate is calculated as follows: 100 × (cfus before incubation − cfus after incubation)/cfus before incubation.

Detection of ROS. ROS production was measured by a luminol-dependent chemiluminescence assay in the absence and presence of exogenously added horseradish peroxidase (HRP) (for intracellular and total ROS, respectively). To measure total ROS production after *N*-Formyl-Met-Leu-Phe (fMLP) stimulation, prewarmed fMLP (5 μM; Sigma-Aldrich) was added with luminol (100 μM; Sigma-Aldrich) and HRP (20 units/mL; Sigma-Aldrich) at the same time and measurement started immediately. ROS production was monitored every 10 s for 5 min with a luminometer. In the bacteria stimulation assay, cells were incubated with luminol in the absence or presence of HRP for 10 min at 37 °C, followed by stimulation with *L. monocytogenes* (MOI = 10). ROS production was monitored every 10 min for 2 h.

Intracellular ROS was also detected using 2′,7′-dichlorofluorescein diacetate (DCFDA) (Sigma-Aldrich). Neutrophils were primed with 10 ng/mL GM-CSF (R&D Systems) for 30 min at 37 °C and then incubated with the fluorogenic probe DCFDA for 30 min. cells were treated with HBSS or 1 μM fMLP for 15 min at 37 °C. ROS was determined on the basis of the fluorescence intensity by flow cytometry. To measure ROS induced by bacteria, cells were infected with *L. monocytogenes* at the ratio of 10:1 for 15 min and incubated for 15 min with 10 μM DCFDA.

ELISA. Sera were collected from *Tipe2*$^{+/+}$ and *Tipe2*$^{-/-}$ mice 24 h after *Listeria* infection and kept at −80 °C. Antibodies used in ELISA were purchased from BD Pharmingen and eBioscience, including purified and biotinylated rat anti-mouse IL-6 and IFNγ. Quantitative ELISA was performed using paired mAbs specific for corresponding cytokines according to the manufacturer's recommendations.

Statistical Analyses. The differences in mRNA, cytokines, phagocytosis, bacterial killing, DCFH, and ROS were analyzed by two-tailed Student's *t* test. The differences in survival rate were

analyzed by a Mann–Whitney *U* test. Statistical analyses were performed on pooled data, and statistics and error bars shown are for independent experiments and not for replicates within a single experiment.

1. Cook DN, Pisetsky DS, Schwartz DA (2004) Toll-like receptors in the pathogenesis of human disease. *Nat Immunol* 5:975–979.
2. Broad A, Jones DE, Kirby JA (2006) Toll-like receptor (TLR) response tolerance: A key physiological "damage limitation" effect and an important potential opportunity for therapy. *Curr Med Chem* 13:2487–2502.
3. Blander JM, Medzhitov R (2004) Regulation of phagosome maturation by signals from toll-like receptors. *Science* 304:1014–1018.
4. Takeda K, Akira S (2005) Toll-like receptors in innate immunity. *Int Immunol* 17:1–14.
5. Kong L, Ge BX (2008) MyD88-independent activation of a novel actin-Cdc42/Rac pathway is required for Toll-like receptor-stimulated phagocytosis. *Cell Res* 18: 745–755.
6. Tricker E, Cheng G (2008) With a little help from my friends: Modulation of phagocytosis through TLR activation. *Cell Res* 18:711–712.
7. Henneke P, et al. (2002) Cellular activation, phagocytosis, and bactericidal activity against group B streptococcus involve parallel myeloid differentiation factor 88-dependent and independent signaling pathways. *J Immunol* 169:3970–3977.
8. Diebold BA, Bokoch GM (2005) Rho GTPases and the control of the oxidative burst in polymorphonuclear leukocytes. *Curr Top Microbiol Immunol* 291:91–111.
9. Dovas A, Couchman JR (2005) RhoGDI: Multiple functions in the regulation of Rho family GTPase activities. *Biochem J* 390:1–9.
10. Boulter E, Garcia-Mata R (2010) RhoGDI: A rheostat for the Rho switch. *Small GTPases* 1:65–68.
11. Harding MA, Theodorescu D (2010) RhoGDI signaling provides targets for cancer therapy. *Eur J Cancer* 46:1252–1259.
12. Rivero F, et al. (2002) Defects in cytokinesis, actin reorganization and the contractile vacuole in cells deficient in RhoGDI. *EMBO J* 21:4539–4549.
13. Yin L, Schwartzberg P, Scharton-Kersten TM, Staudt L, Lenardo M (1997) Immune responses in mice deficient in Ly-GDI, a lymphoid-specific regulator of Rho GTPases. *Mol Immunol* 34:481–491.
14. Bielek H, Anselmo A, Dermardirossian C (2009) Morphological and proliferative abnormalities in renal mesangial cells lacking RhoGDI. *Cell Signal* 21:1974–1983.
15. Sun H, et al. (2008) TIPE2, a negative regulator of innate and adaptive immunity that maintains immune homeostasis. *Cell* 133:415–426.
16. Clemens RA, et al. (2004) PRAM-1 is required for optimal integrin-dependent neutrophil function. *Mol Cell Biol* 24:10923–10932.
17. Campbell PA, Canono BP, Drevets DA (2001) Measurement of bacterial ingestion and killing by macrophages. *Curr Protoc Immunol* Chap 14:Unit 14.6.
18. Decleva E, Menegazzi R, Busetto S, Patriarca P, Dri P (2006) Common methodology is inadequate for studies on the microbicidal activity of neutrophils. *J Leukoc Biol* 79: 87–94.

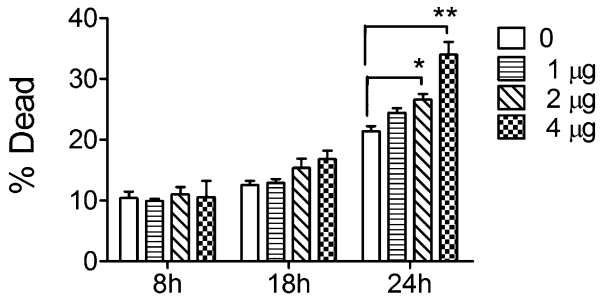

Fig. S1. Cell death in TIPE2-overexpressing 293T cells. 293T cells were transfected with the indicated amounts of Flag-TIPE2 construct. Cell death was assessed by trypan blue staining. Data shown are mean± SEM (n = 4) of three independent experiments. *P < 0.05; **P < 0.01.

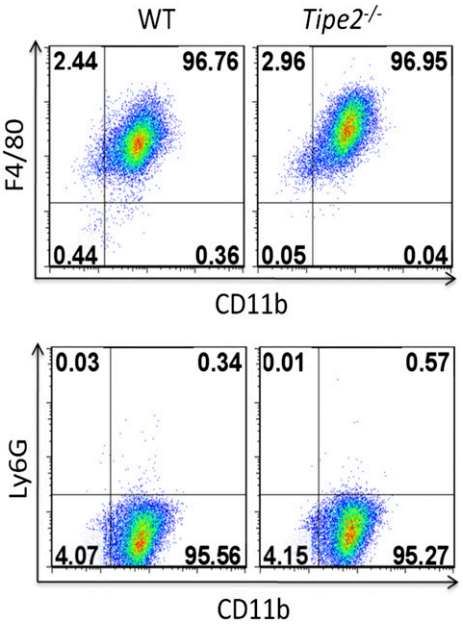

Fig. S2. The phenotypes of BMDMs. BMDMs from WT and *Tipe2*$^{-/-}$ mice were stained with anti-mouse CD11b, F4/80, and Ly6G and then analyzed by flow cytometry.

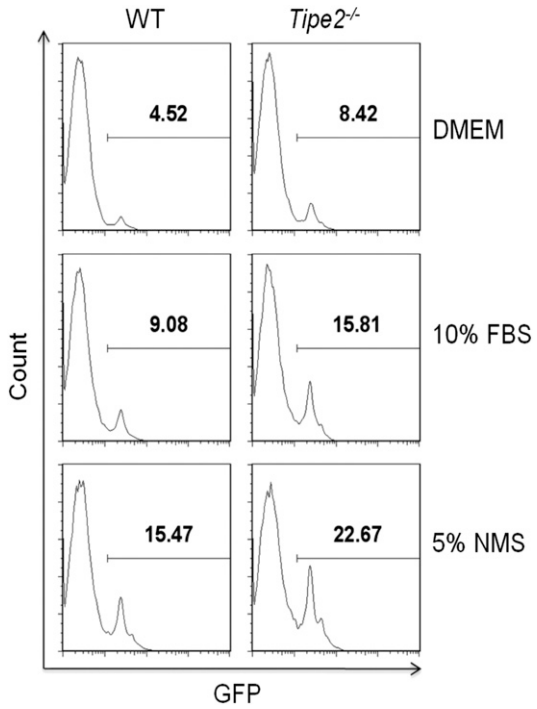

Fig. S3. Phagocytosis in different media. WT and *Tipe2*$^{-/-}$ BMDMs were subjected to the phagocytosis assay as in Fig. 5*A*, in (*Top*) DMEM without sera (DMEM), (*Middle*) DMEM with 10% heat-inactivated FBS (10% FBS), and (*Bottom*) DMEM with 5% fresh normal mouse sera (5% NMS).

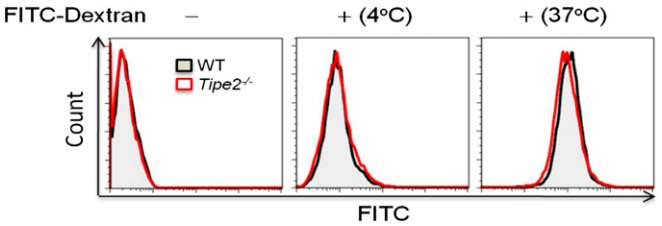

Fig. S4. Endocytosis of dextrans. BMDMs from WT and *Tipe2*$^{-/-}$ mice were incubated with or without 1 mg/mL FITC-labeled dextran (Invitrogen) in PBS containing 1% BSA, for 30 min at 4 °C or 37 °C. After the incubation, cells were washed five times and analyzed by flow cytometry.

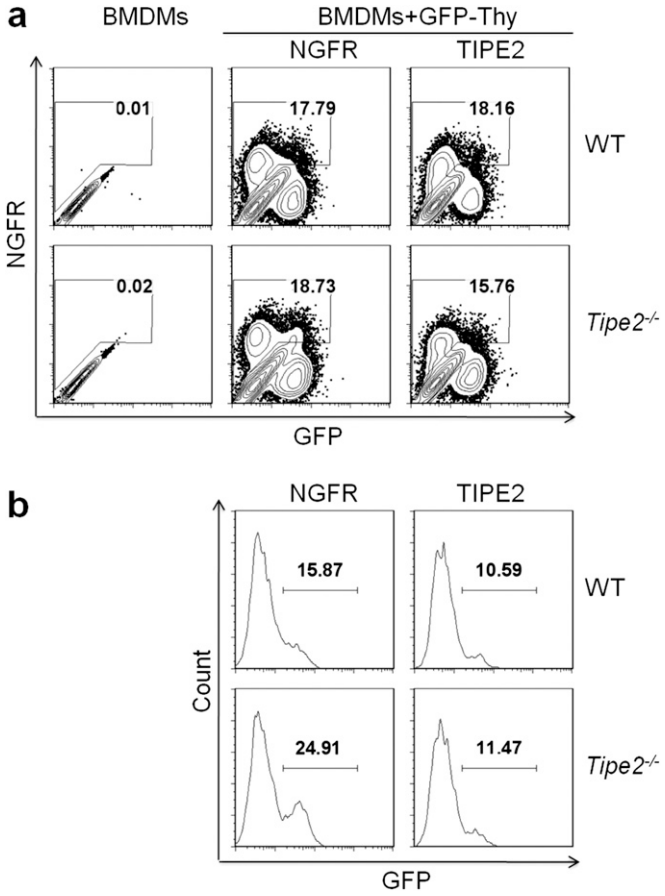

Fig. S5. TIPE2 inhibits phagocytosis. BMDMs were treated and tested as in Fig. 5*D*. (*A*) Each number represents the percentage of NGFR$^+$ cells in macrophages. (*B*) Each number represents the percentage of GFP$^+$ cells in NGFR$^+$ macrophages. Results are representative of three independent experiments.

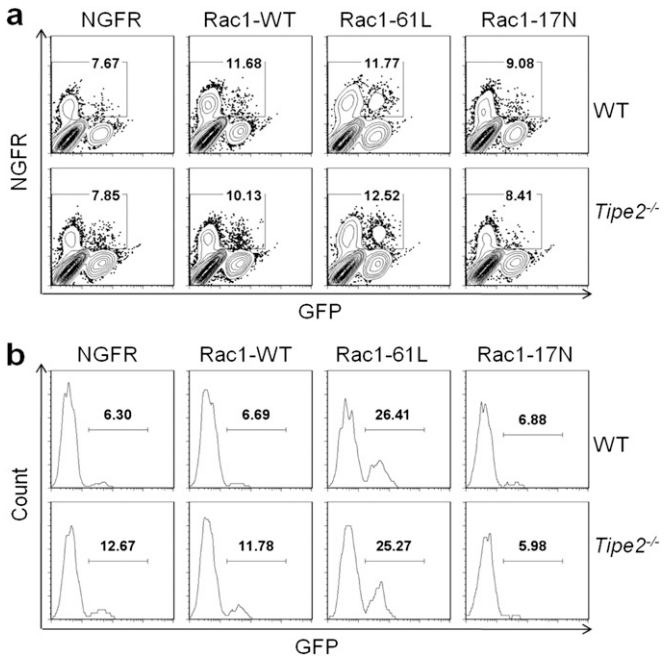

Fig. S6. TIPE2 inhibits phagocytosis through Rac. BMDMs were treated and tested as in Fig. 5*E*. (*A*) Each number represents the percentage of NGFR$^+$ cells in macrophages. (*B*) Each number represents the percentage of GFP$^+$ cells in NGFR$^+$ macrophages. Results are representative of three independent experiments.

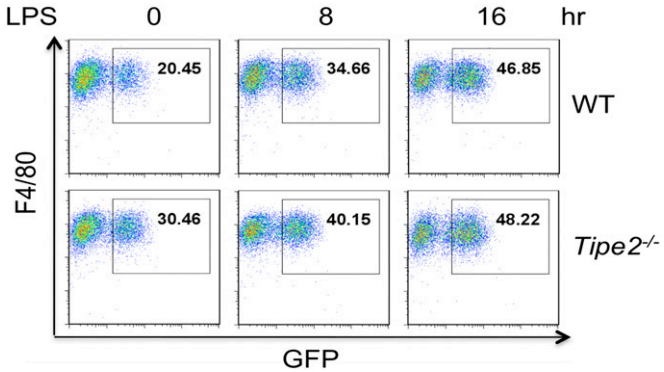

Fig. S7. LPS-induced increase in phagocytosis is diminished in TIPE2-deficient cells. BMDMs were treated and tested as in Fig. 5*G*. Each number represents the percentage of GFP$^+$ cells in the macrophages.

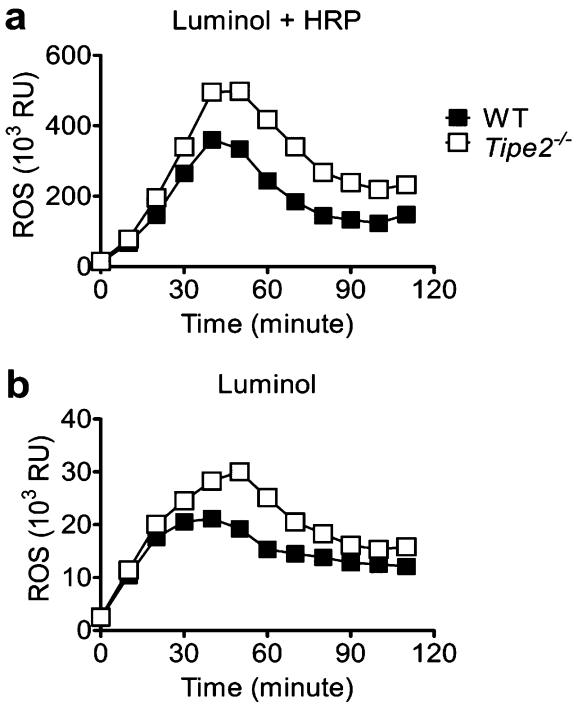

Fig. S8. Oxidative burst in neutrophils. Bone marrow neutrophils from wild-type and *Tipe2*$^{-/-}$ mice were analyzed for *Listeria*-induced ROS production, using the Luminol assay. The assay was performed in the presence (*A*) and absence (*B*) of exogenously added HRP to measure total and intracellular ROS, respectively. RU, relative units.